Appl Biochem Biotechnol (2009) 158:59–71
DOI 10.1007/s12010-008-8302-4

Expression Analysis and Characteristics of *Profilin* Gene from Silkworm, *Bombyx mori*

Zuoming Nie · Jiangtao Xu · Jian Chen · Zhengbing Lv · Dan Wang · Qing Sheng · Yi Wu · Xuedong Wang · Xiangfu Wu · Yaozhou Zhang

Received: 13 April 2008 / Accepted: 17 June 2008 /
Published online: 17 July 2008

Abstract A recombinant *Bombyx mori* profilin protein (rBmPFN) was overexpressed in *Escherichia coli* BL21. Purified rBmPFN was used to generate anti-BmPFN polyclonal antibody, which were used to determine the subcellular localization of BmPFN. Immunostaining indicated that profilin can be found in both the nucleus and cytoplasm but is primarily located in the cytoplasm. Real-time RT-PCR and Western blot analyses indicated that, during the larvae stage, profilin expression levels are highest in the silk gland, followed by the gonad, and are lowest in the fatty body. Additionally, BmPFN expression begins during the egg stage, increases during the larvae stage, reaches a peak during the pupa stage, and decreases significantly in the moth. Therefore, we propose that BmPFN may play an important role during larva stage development, especially in the silk gland.

Keywords Profilin · Expression analysis · Subcellular localization · Real-time PCR · *Bombyx mori*

Introduction

Profilin, which has a highly conserved structure and function, was one of the first actin-binding proteins identified [1]. It plays an important role in many important cellular processes, including membrane trafficking [2], GTPase signal transduction [3, 4], transcription regulation [5, 6], RNA splicing [7–10], neurological genesis and differentiation [11–14], and tumor formation [15]. It also plays an important role in the polarity of plant cell growth in pollen tubes and root hairs [16]. Plant profilins have been identified in

Z. Nie · J. Xu · J. Chen · Z. Lv · D. Wang · Q. Sheng · Y. Wu · X. Wang · X. Wu · Y. Zhang (✉)
Institute of Biochemistry, College of Life Sciences, Zhejiang Sci-Tech University,
Xiasha High-Tech Zone No.2 Road, Hangzhou 310018, China
e-mail: yaozhou@chinagene.com

pollen and have also been implicated in food allergies [17–19]. Typically, higher organisms express multiple profilin isoforms having similar structures, but different ligand binding affinities and expression patterns, indicating that they play different roles in vivo [20–26]. Currently, most studies focus on determining the effects of profilin overexpression or inhibition, identifying new ligands, and determining the mechanisms that regulate profilin function and expression [21–26].

Insect profilins have been studied mainly in *Drosophila.* Cooley et al. found that the *Drosophila* profilin gene (*chickadee*) has two promoters, one that is specifically active in the ovary and another that is active in all tissues [27]. Verheyen et al. found that a genomic deletion of the *chickadee* locus ($pfn^{ko/ko}$) results in an embryonic lethal phenotype. Although $pfn^{ko/wt}$ mutants survive, serious developmental defects occur during oogenesis, spermatogenesis, and bristle formation. Mitosis is also seriously affected in this mutant [28]. Minakhina et al. found that profilin and actin-filaments play important roles in nuclear trafficking and that the localization of the nuclear exporting regulation protein Ran GAP (Ran GTPase activating protein) is controlled by profilin [29]. However, no studies on silkworm profilin or profilin in any other Lepidoptera has been reported, and no physical or chemical information on the silkworm profilin protein is currently available.

In this study, we identified a silkworm profilin complementary DNA (cDNA; *BmPFN*) from a pupal cDNA library (GenBank Accession: EF112402). Using bioinformatics analysis, we have determined the evolutionary relationship and degree of conservation between BmPFN and other profilin orthologs. We have also used immunohistochemistry, real-time RT-PCR, and Western blot analyses to determine the subcellular localization, expression levels, and tissue distribution of BmPFN during the various silkworm developmental stages. Our results provide a solid foundation on which to base further research on the developmental and functional roles played by profilin in the silkworm.

Materials and Methods

Materials

The *Bombyx mori* strain used in this study is Qingsong × Haoyue. The head, fatty body, intestine, martensite, gonad, silk gland, skin, and trachea from fifth instar larvae were dissected, frozen immediately in liquid nitrogen, and stored at −80°C. Nascent eggs, pupae (3 days after pupation), each instar larvae, and moths were also frozen in liquid nitrogen and stored at −80°C. 4′-6-Diamidino-2-phenylindole (DAPI) was purchased from Sigma. Cy3-labeled goat anti-rabbit IgG was purchased from Proteintech Group Inc. *Bm5* cells (a gift from Prof. Zhi-Fang Zhang) were cultured in TC-100 medium (Sigma) supplemented with 10% fetal calf serum (FCS, Gibco BRL) at 27°C. The One-Step SYBRGreen Kit was purchased from Invitrogen.

Bioinformatics Analysis

The *BmPFN* gene was identified in the process of analyzing the cDNA sequences from the *B. mori* pupa cDNA library constructed by our laboratory [30]. Genomic structure for this gene was analyzed by comparing the cDNA sequence with corresponding genomic DNA sequences downloaded from the Beijing Genomics Institute (http://silkworm.genomics.org.cn). The similarity analysis of nucleotide and protein sequences was performed using the BLAST algorithm from NCBI (http://www.ncbi.nlm.nih.gov/). The characteristics of this

gene were analyzed using DNAstar software. The orthologous sequences used for multiple sequence alignments were obtained from NCBI. Softwares used for alignments were Clustal W and BioEdit ver. 7.01. The software used for phylogenetic tree analysis was phyml ver. 2.4.4. The positions, in which the amino acid residues identities between orthologs were more than 90%, were shown with shadow. We used phyml ver. 2.4.4 to construct a phylogenetic tree by applying results determined by multiple sequence alignments using a maximum-likelihood method; the bootstrap was set to 1,000 [31]. The predicted three-dimensional structure of BmPFN was generated by SWISS-MODEL (http://swissmodel.expasy.org//SWISS-MODEL.html) [4, 32].

Expression, Purification, and Antibody Preparation of Recombinant BmPFN

The BmPFN ORF was subcloned into the prokaryotic expression vector pGEX-5x-1. *Escherichia coli* BL21 (DE3) were transformed with the recombinant plasmid, the transformed *E. coli* were grown in culture, and recombinant protein expression was induced with IPTG. The recombinant fusion protein GST-BmPFN was extracted from the bacteria and purified using GST Trap FF (1 ml) column chromatography. Purified GST-BmPFN was digested with Factor-Xa, and the rBmPFN was used to generate anti-BmPFN polyclonal antibody in a New Zealand rabbit. Antiserum from the immunized rabbit was passed through a Protein A HP chromatography column to obtain purified rabbit IgG. An ELISA was used to determine the polyclonal antibody titer, and the specificity of the polyclonal antibody was determined by Western blot analysis (the purified polyclonal antibody was diluted 1:4,000 and incubated with the immunoblot at room temperature for 2 h; the goat anti-rabbit secondary antibody was diluted 1:1,000).

Subcellular Localization of BmPFN

Cells were cultured overnight on glass cover slips, washed for 10 min three times in PBS, and fixed (PBS, pH 7.2, 4% poly-formaldehyde, 0.1% Triton X-100) at room temperature for 15 min. The fixed cells were blocked in 3% BSA in PBS at room temperature for 2 h followed by three 10-min washes in PBST (0.05% Tween-20 in PBS). Cells were then incubated with antiserum containing anti-BmPFN polyclonal antibody (diluted 1:200 in blocking buffer) at 4°C overnight; cells were simultaneously incubated with negative serum as a control. The negative serum was obtained from the rabbit before immunizing with antigen. After three 10-min washes in PBST, cells were incubated with Cy3-labeled goat anti-rabbit IgG (diluted 1:500; Promega) at 37°C for 2 h and were then washed twice for 10 min in PBST. Cells were then incubated with 4′-6-diamidino-2-phenylindole (1 g/ml in PBS) at room temperature for 10 min. After washing once with PBST, cells were examined under a Nikon ECLIPSE TE2000-E Confocal Microscope; images were analyzed using EZ-C1software.

RNA Extraction

Total RNA from various silkworm development stages and fifth instar larvae tissues (see "Materials") was isolated using Trizol (Invitrogen) according to manufacturer's instructions. Contaminating genomic DNA was removed by DNase I (Invitrogen). The purity of extracted RNA was determined by UV spectrophotometer ND-1000 (NanoDrop). Ratios of UV 260/280 were between 1.8 and 2.1 for all RNA samples analyzed. The concentration of total RNA was determined by measuring the absorbance at 260 nm.

Expression Analysis of BmPFN by Real-Time RT-PCR

The primers used in the real-time RT-PCR were designed using the Primerselect program from the DNAstar software package. A pair of primers was designed for amplifying 18S ribosomal RNA (rRNA), which was used as an internal control. The sequences of primers used in the RT-PCR are as follows:

18 s rRNA: Forward primer, 5'CGATCCGCCGACGTTACTACA3';
Reverse primer, 5'GTCCGGGCCTGGTGAGATTT3'.
BmPFN: Forward primer, 5'GTGTGGGCAAAGTCGGAAGG3';
Reverse primer, 5' GCGCGGATGATATGGTCTGTG3'.

The RT-PCR was performed in an ABI Prism 7300 Sequence Detection System (Applied Biosystems); SuperScript™ III Platinum® SYBR® Green One-Step qRT-PCR Kit with ROX (Invitrogen) was used for real-time PCR. Reaction mixtures (15 μl) contained 7.5 μl 2× SYBR-Green Reaction mixed with Rox, 0.3 μl Superscript™ III RT/platinum® Taq mix, 1.2 μl 1 μM forward and reverse primers, respectively, 1 μl total RNA and 3.8 μl DEPC-water. Reaction parameters used in the real-time RT-PCR were, for reverse transcription, 50°C for 3 min; for pre-denaturation, 95°C for 5 min; PCR cycles, 95°C for 15 s, 59°C for 15 s, 72°C for 30 s, 40 cycles. The dissociation curve was determined using the following parameters: 95°C for 15 s, 60°C for 30 s, 95°C for 15 s, to check for the presence of non-specific dsDNA SYBR Green hybrids such as primer-dimers. In a 96-well plate, each reaction was performed in triplicate along with the endogenous 18S rRNA control gene.

Expression levels of the target genes were normalized against the expression level of the 18S rRNA gene. Relative expression levels were calculated using $2_{\mathrm{T}}^{-\Delta\Delta C}$ method for RNA quantification where $\Delta\Delta C_{\mathrm{T}}=(C_{\mathrm{T}}$, target gene$-\mathrm{C_T}$, 18S rRNA$)_{\text{different stages or tissues}}-(C_{\mathrm{T}}$, target gene$-C_{\mathrm{T}}$, 18S rRNA$)_{\text{maximum}}$ [33, 34].

Expression Analysis of BmPFN by Western Blot

To prepare protein extracts, silkworm stages or tissues were frozen in liquid nitrogen, ground to a fine powder, and treated with protein extraction lysate buffer (50 mM Tris pH 8.0, 0.15 M NaCl, 5 mM EDTA, 0.5% NP-40, 1 mM dithiothreitol, 5 g/l sodium deoxycholate, 100 mg/l PMSF, 5 μg/ml Aprotin). After 30 min on ice, homogenates were centrifuged at 12,000×*g* for 15 min at 4°C. Proteins in the supernatant were separated by SDS-PAGE in a 12% gel and then electrotransferred onto PVDF membranes (Millipore). Protein concentrations in the samples were determined using the Bradford method and equalized prior to SDS-PAGE. Quantitative analysis was performed by Bandscan 5.0 software.

Results

Bioinformatics Analysis

We obtained a unique cDNA that encodes a protein containing 126-amino acid and having a predicted molecular weight of 13.71 kDa. This protein was identified as *B. mori* profilin, which contains a domain that is conserved (cd00148, PROF) in other known profilin proteins. We named this protein BmPFN (GenBank accession: ABK97428). This gene, *BmPFN*, contains three exons and four introns (Fig. 1a). Although function is highly

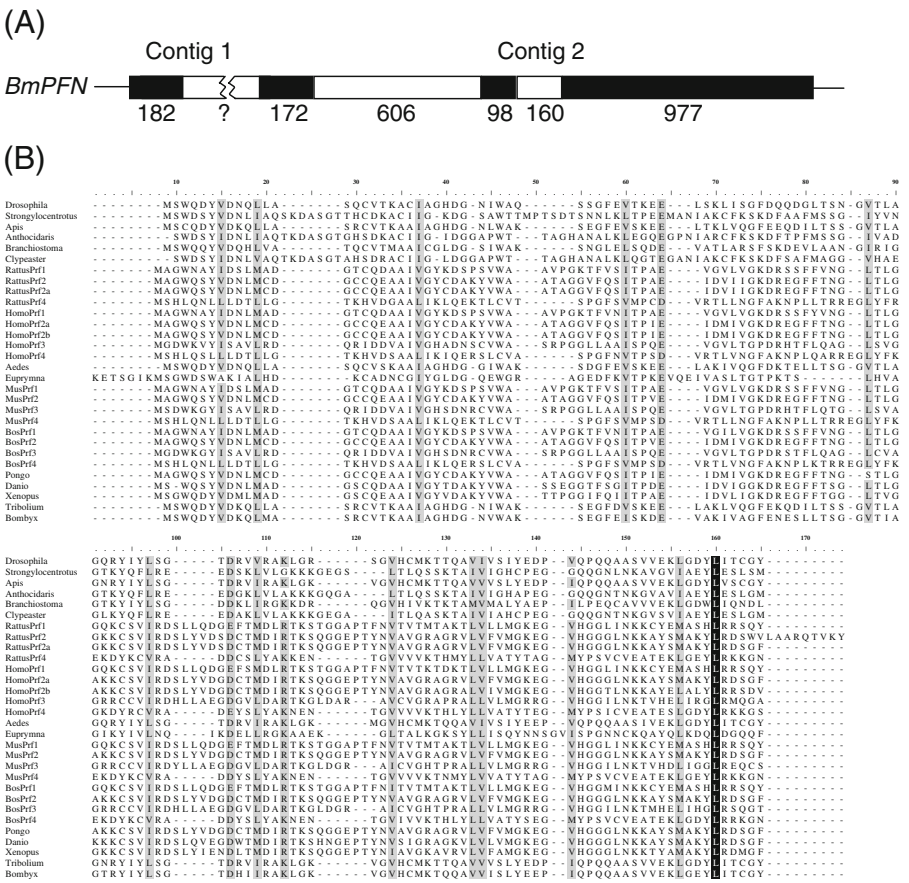

Fig. 1 Bioinformatics analysis of the silkworm *BmPFN* gene. **a** A schematic representation of the silkworm *BmPFN* gene. This gene contains three introns and four exons and is located in two contigs of silkworm genome (Contig1: AADK01003437.1; Contig 2: AADK01012064.1). Exons are indicated as *black boxes* and introns as *white boxes*. The *number of bases* above each box indicate the exons' and introns' size; **b** multiple sequence alignment of animal profilins. The conserved positions were indicated with *shade*

conserved among members of the profilin protein family, sequence similarities between profilins from invertebrate and vertebrate species are low (ranged from 15% to 31%). Only the C- and N-terminus are relatively conserved in animal profilin, and L121 is conserved in the C-terminus of all animal sequences that were analyzed (Fig. 1b). Interestingly, BmPFN and mammalian profilin IV isoforms cluster together in a group in the phylogenetic tree with the profilins from some insects (e.g., *Aedes aegypti*, *Drosophila melanogaster*, *Apis mellifera*, and *Tribolium castaneum*; Fig. 2). Structure predictions indicate that BmPFN has a three-dimensional conformation that is extremely similar to that of other profilins. It is comprised of three α-helices and seven beta-folds; a combination of an N-terminus α-helix (α1) and a C-terminus α-helix (α3) secures the seven beta-folds like a clamp, while the remaining α-helix (α2) resides on the other side of the protein (data not shown).

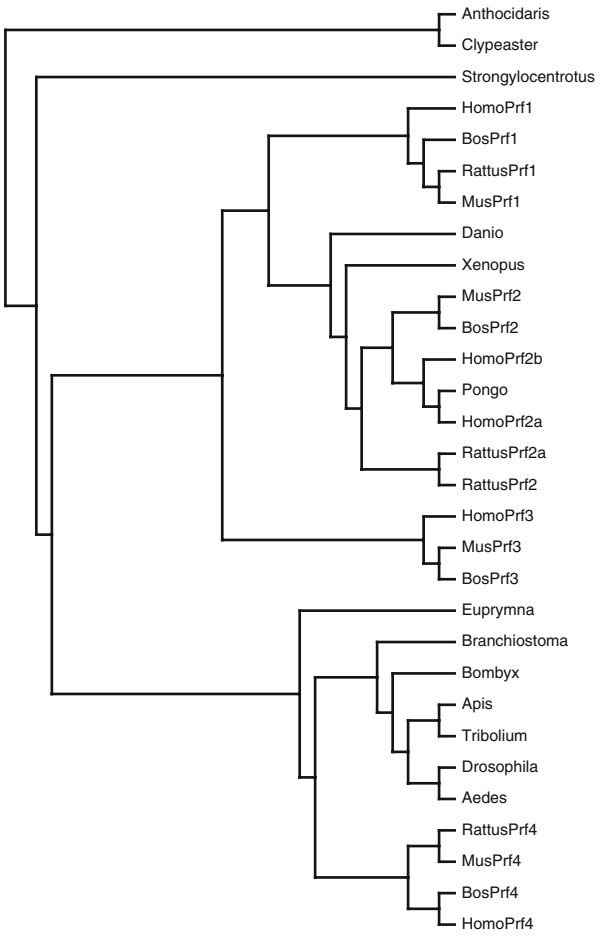

Fig. 2 Phylogenetic tree of animal profilins

Prokaryotic Expression of BmPFN and Preparation of Polyclonal Antibody

The *BmPFN* ORF was subcloned into the *Eco*RI and *Not*I restriction sites of the pGEX-5x-1 expression vector. *E. coli* BL21 (DE3) transformed with the recombinant plasmid were grown in culture, and recombinant fusion protein expression (GST-BmPFN) was induced by IPTG. The predicted molecular weight of BmPFN is 13.7 kDa, and the molecular weight of the GST label is 26 kDa. The molecular weight of the fusion protein GST-BmPFN, as determined by electrophoresis, is 40 kDa, which is consistent with the calculated value (Fig. 3). Using digested and purified fusion protein rBmPFN, anti-BmPFN polyclonal antibody was generated in an immunized New Zealand rabbit and was purified by Protein A HP column chromatography (Amersham). The anti-BmPFN polyclonal antibody titer, as determined by ELISA, was 1:32,000, and Western blot analysis indicated that the antibody reacted specifically with GST-BmPFN (Fig. 3).

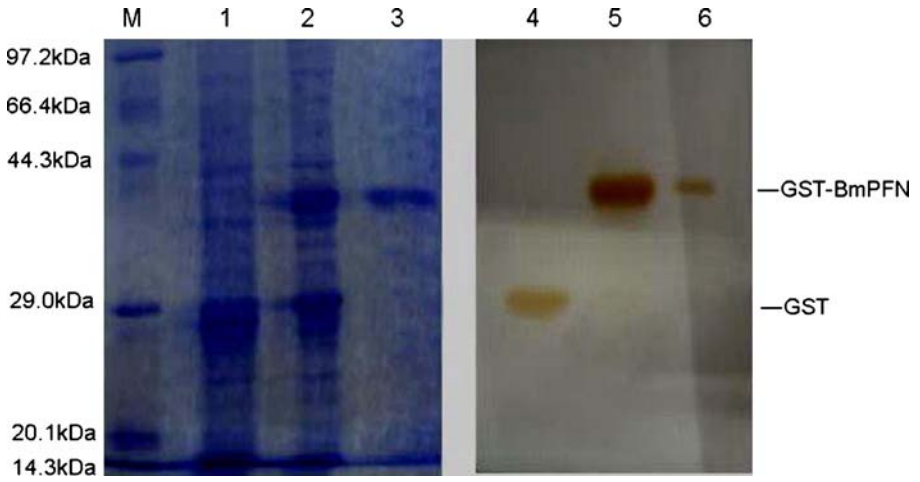

Fig. 3 Purification of the fusion protein GST-BmPFN and Western blot analysis of the specificity of antiserum. *M* Low molecular weight protein marker, *1* protein from uninduced BL21(DE3)-pGEX-5x-1-BmPFN, *2* protein from BL21-pGEX-5x-1 after inducing with IPTG, *3* purified fusion protein GST-BmPFN, *4* GST control, *5* total protein from *E. coli* BL21-pGEX-5x-1-BmPFN induced with IPTG, *6* purified fusion protein GST-BmPFN

Subcellular Localization of BmPFN

The treated cells were examined under a Nikon ECLIPSE TE2000-E Confocal Microscope, and images were analyzed using EZ-C1software. Cy3-labeled goat anti-rabbit IgG emits red fluorescence when stimulated with light having a wavelength of 550 nm, and DAPI-stained nuclei emit red fluorescence when stimulated with light having a wavelength of 353 nm. Our results indicate that BmPFN is located in both the cytoplasm and nucleus but is primarily found in the cytoplasm (Fig. 4).

Expression Analysis of BmPFN

We employed real-time RT-PCR to quantify *BmPFN* messenger RNA (mRNA) levels during the various stages of silkworm development and in fifth instar larvae tissues, including the head, fatty body, intestine, martensite, gonad, silk gland, skin, and trachea. Data analysis was performed using ABI Prism 7300 SDS Software V1.3.1 (Applied Biosystems, USA). For real-time PCR analyses, we used a constitutively expressed gene, 18S rRNA, as an internal control. For *BmPFN* and 18S rRNA of silkworm, dissociation curves indicated proper amplification of the intended targets at the corresponding melting temperatures (data not shown). The PCR efficiencies estimated is near 100%. Our results indicate that BmPFN expression is higher in larvae and lower in egg (Fig. 5). In larva tissues, BmPFN expression is higher in the silk gland and lower in the fatty body (Fig. 6). At the same time, we used Western blot analyses to determine BmPFN protein levels in total protein extracts from egg, each instar larvae, pupa, and moth. The results showed that BmPFN expression was difficult to detect in the egg and in the first instar larvae but increased during development from the second instar larvae to the pupa. Its expression level

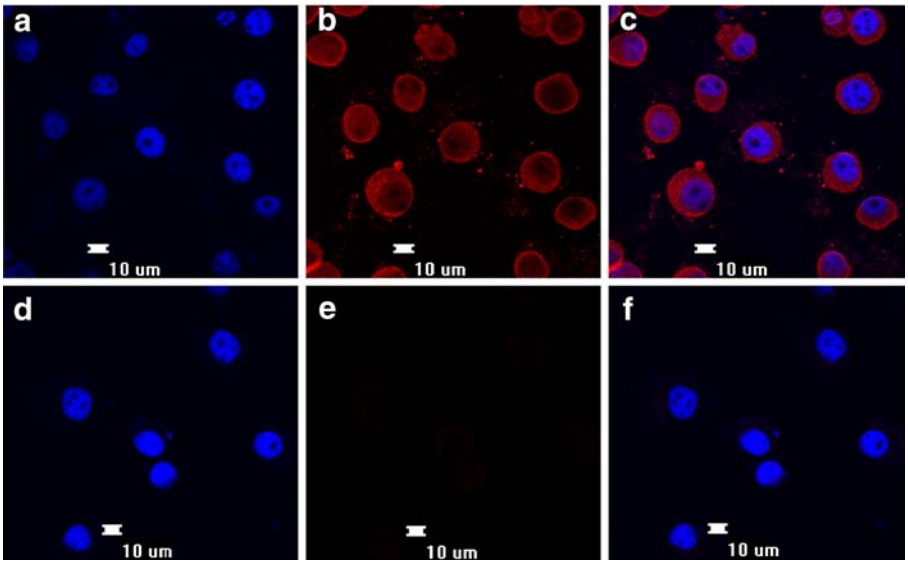

Fig. 4 Subcellular localization of BmPFN with Cy3-labled goat ant-rabbit IgG and DAPI. **a**–**c** Experimental group, using anti-BmPFN polyclonal antibody. **a** DAPI staining; **b** BmPFN subcellular localization as indicated by Cy3-labeled secondary antibody; **c** merged image of **a** and **b**; **d**–**f** negative control group, using negative rabbit serum; **d** DAPI staining; **e** Cy3-labeled secondary antibody; **f** merged image of **d** and **e**

was highest in the pupa, moderated between the fourth instar and fifth instar larvae, and decreased significantly in the moth (Fig. 7). Comparing with the mRNA and protein levels, we can see that the protein level is not consistent with the mRNA level during development. The larvae stage contained the highest mRNA level, but the highest protein level was observed in pupa stage.

Discussion

Multiple sequence alignments of profilin proteins from various species revealed that profilin amino acid sequences are highly conserved only in the C- and N-terminus. The leucine L121, which is conserved in the C-terminus of all the profilin sequences examined, contributes to the C-terminus α-helix, which, together with the N-terminus α-helix, forms

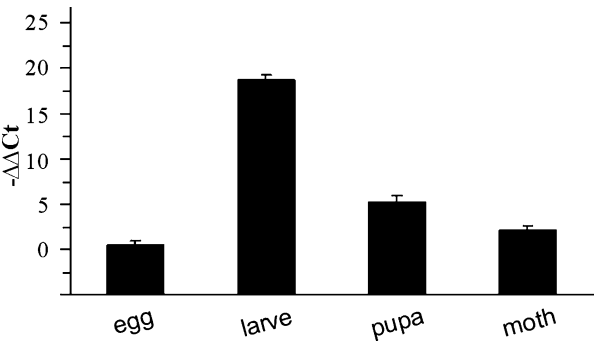

Fig. 5 Expression levels of BmPFN in different silkworm developmental stages. Relative expression level of BmPFN was identified by real-time PCR. The relative expression level was calculated by using $2_{T}^{-\Delta\Delta C}$, where $\Delta\Delta C_T=(C_T$, target gene$-C_T$, 18S rRNA$)_{\text{different stages}}-(C_T$, target gene, 18S rRNA) eggs

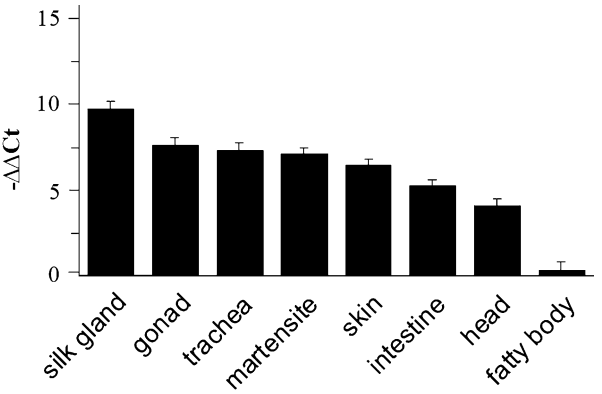

Fig. 6 Expression levels of BmPFN in different tissues of fifth instar larvae. The relative expression level was calculated by using $2_{\mathrm{T}}^{-\Delta\Delta C}$, where $\Delta\Delta C_{\mathrm{T}}$= ($C_{\mathrm{T}}$, target gene−$C_{\mathrm{T}}$, 18S rRNA)$_{\text{different tissues}}$−($C_{\mathrm{T}}$, target gene, 18S rRNA) fat bodies

the poly-L-proline-binding site [35, 36]. The phylogenetic analysis showed that BmPFN has a closest phylogenetic relationship with insect profilins; however, profilin IV is also highly related to BmPFN. This is consistent with the description by Polet et al. that profilin IV is most related to invertebrate profilins and originated prior to vertebrate evolution, whereas separation of profilins I, II, and III isoforms occurred early in vertebrate evolution [37]. The tree also showed that BmPFN and profilin IV could evolve from a common ancestor similar to sea urchin profilin. Furthermore, although the identities of the full-length amino acid sequences are low, their tertiary structures are highly conserved, showing that very different sequences can form similar structures. The ATPase active sites found in actin [38] and heat shock proteins [39] are other excellent examples of different amino acid sequences forming similar structures.

In the *Bm5* cell line, BmPFN is found primarily in the cytoplasm but is also observed in the nucleus. Profilin regulates actin polymerization and depolymerization [1, 40–41] and also acts as a control hub for a network of molecular interactions [20, 42]. Therefore, it is not difficult to understand the ubiquitous distribution of this protein throughout the cytoplasm. It has been previously reported that profilin can be found in the nucleus [7, 43–45]. It is possible that profilin and actin play important roles in RNA splicing, chromosome remolding, and transcriptional regulation. Although the function of actin in the nucleus is not clear, the existence of a nuclear microfilament component suggests a role in nucleus–cytoplasm dynamics. Profilin may bind transcriptional regulators as well and has been shown to regulate transcription by affecting the activity of p42$^{\mathrm{POP}}$ [5]. Furthermore, profilin and the actin cytoskeleton also play important roles in nuclear transport [29]. In an experiment designed to determine profilin distribution during the cell cycle, Vaster et al.

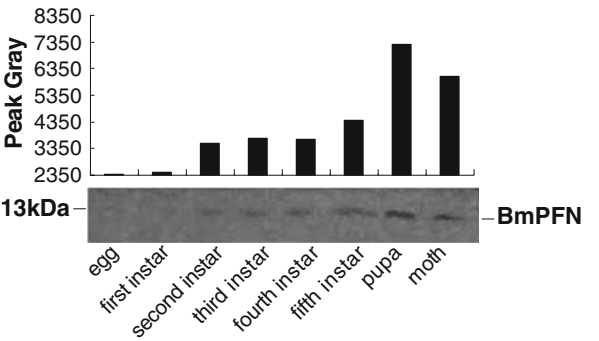

Fig. 7 Western blot analysis of the expression levels of BmPFN during different silkworm developmental stages

found that profilin specifically accumulates in the nucleus in interphase and prophase cells, and profilin distribution in the nucleus is dependent on the nuclear matrices and nuclear envelopes [43]. However, the details and significance of the role of profilin and actin polymerization–depolymerization dynamics in the nucleus remain unclear.

Our real-time RT-PCR and Western blot analyses showed that BmPFN expression begins during the egg stage, increases during the larvae stage, and decreases in the moth. However, minor differences in the results obtained by RT-PCR and Western blot analyses were also observed. Real-time RT-PCR showed that *BmPFN* expression peaked in the larvae, but

Table 1 The putative binding sites in *Bombyx mori profilin* to microRNAs.

MicroRNAs and position of putative binding sites in *profilin*	Binding between *profilin* and microRNAs
miRNA: bmo-mir-2a-1[a]	Target 5′ C GG ACUG U 3′
Position: 1396	UGAUAAGCCGAU GA UGUC
	ACUGUUUGGCUG CU ACGG
	miRNA 3′ AU AAA 5′
miRNA: bmo-mir-31	Target 5′ U UUGUUUUUA G 3′
Position: 1183	GCUAUGCU UUUUUGCC
	CGAUACGG AAGAACGG
	miRNA 3′ GU CUG 5′
miRNA: bmo-mir-34	Target 5′ A G GGCAGCGCAG G 3′
Position: 1120	GCACAA CGGC GACU CGC GCC
	UGUGUU GUCG UUGG GUG CGG
	miRNA 3′ A G A U A 5′
miRNA: bmo-mir-305[a]	Target 5′ C AAUUUACA AGC G G 3′
Position: 1105	GUGUG UCCA ACAAGCG C
	CACAU AGGU UGUUCGC G
	miRNA 3′ U G G AC 5′
miRNA: bmo-mir-87	Target 5′ C A C A A 3′
Position: 1015	AUACAUCU AGGG UUGUU CA
	UGUGUGGA UUUC AACGA GU
	miRNA 3′ C A 5′
miRNA: bmo-mir-34	Target 5′ A AAA A U GAU U 3′
Position: 879	GCACA ACCGGU UAGCU CAU UGUU
	UGUGU UGGUCG AUUGG GUG ACGG
	miRNA 3′ A U 5′
miRNA: bmo-mir-210	Target 5′ A CAGUUGG A A 3′
Position: 857	AGCUGUUGUU ACAU GCACAA
	UCGGCGACAG UGUG CGUGUU
	miRNA 3′ 5′
miRNA: bmo-mir-317	Target 5′ G A U G 3′
Position: 850	ACUGCU AGCUG UGUUCA
	UGGUGG UCGAC ACAAGU
	miRNA 3′ CUA GA 5′
miRNA: bmo-bantam	Target 5′ U G C A 3′
Position: 758	UUAGCUUU CAUAG UGAUCUCA
	AAUCGAAA GUGUU ACUAGAGU
	miRNA 3′ UU 5′

[a] A total of nine binding sites were found. The data about the new *Bombyx mori* microRNAs will be published elsewhere.

Western blot analysis showed that expression peaked during the pupa stage. Our results showed that the expression of BmPFN is translationally downregulated. Previously, studies suggested that the expressions of genes can be regulated at translational level by translation regulators such as RBPs [46, 47] and microRNA. MicroRNA can repress mRNA translation by binding the 3′ UTR of targeted gene mRNA and thus downregulate the expression of protein [48–51]. Post-transcriptional silencing of *BmPFN* by microRNAs may be a possible mechanism. The computational analysis also showed that *BmPFN* may be targeted by microRNAs and that the 3′ UTR of *BmPFN* gene contains nine putative microRNA binding sites (Table 1). However, other mechanism could also be existed.

Our results suggest that BmPFN plays important roles during the larvae stage, especially in the fifth instar larvae, but probably does not have an important role in the egg. Our analysis of *BmPFN* mRNA expression in various tissues in the fifth instar larvae showed that its expression level is much higher in the silk gland than in other tissues; the silk gland is in a highly active state during this stage of development. During the pupa stage, the silk gland fades away, while BmPFN expression decreases, indicating a possible relationship between silk gland activity and BmPFN expression. Many reports have shown that profilins play important roles in biologically active cellular compartments [16]. Profilin regulates actin polymerization and depolymerization as well as actin dynamics [1, 40, 41, 52, 53], which play an important role in determining cell shape and movement through the cytoplasm [42]. Since silk protein and sericin are produced by the silk gland, it is possible that BmPFN plays an important role in the synthesis, assembly, or secretion of these important substances.

Acknowledgements This work was supported by financial grants from the National Natural Science Foundation of China (No.30740015), the National High Technology Research and Development Program (No. 2007AA021703, No. 2007AA100504), the National Basic Research Program of China (No. 2005CB121006), and the Zhejiang Natural Science Foundation (No. Y305171).

References

1. Carlsson, L., Nystrom, L. E., Sundkvist, I., et al. (1977). *Journal of Molecular Biology*, *115*, 465–483. doi:10.1016/0022-2836(77)90166-8.
2. Gareus, R., Di Nardo, A., Rybin, V., & Witke, W. (2006). *The Journal of Biological Chemistry*, *281*, 2803–2811. doi:10.1074/jbc.M503528200.
3. Kobayashi, K., Kuroda, S., Fukata, M., et al. (1998). *The Journal of Biological Chemistry*, *273*, 291–295. doi:10.1074/jbc.273.1.291.
4. Schwede, T., Kopp, J., Guex, N., et al. (2003). *Nucleic Acids Research*, *31*, 3381–3385. doi:10.1093/nar/gkg520.
5. Lederer, M., Jockusch, B. M., & Rothkegel, M. (2005). *Journal of Cell Science*, *118*, 331–341. doi:10.1242/jcs.01618.
6. Burke, E., Mahoney, N. M., Almo, S. C., et al. (2000). *Journal of Virology*, *74*, 669–675. doi:10.1128/JVI.74.2.669-675.2000.
7. Skare, P., Kreivi, J. P., Berqstrom, A., et al. (2003). *Experimental Cell Research*, *286*, 12–21. doi:10.1016/S0014-4827(03)00102-2.
8. Giesemann, T., Tathke-Hartlieb, S., Rothkeqel, M., et al. (1999). *The Journal of Biological Chemistry*, *274*, 37908–37914. doi:10.1074/jbc.274.53.37908.
9. Pellizzoni, L., Yong, J., & Dreyfuss, G. (2002). *Science*, *298*, 1775–1779. doi:10.1126/science.1074962.
10. Rossoll, W., Jablonka, S., Andreassi, C., et al. (2003). *The Journal of Cell Biology*, *163*, 801–812. doi:10.1083/jcb.200304128.
11. Neuhoff, H., Sassoe-Pognetto, M., Panzanelli, P., et al. (2005). *The European Journal of Neuroscience*, *21*, 15–25. doi:10.1111/j.1460-9568.2004.03814.x.
12. Da Silva, J. S., Medina, M., Zuliani, C., et al. (2003). *The Journal of Cell Biology*, *162*, 1267–1279. doi:10.1083/jcb.200304021.

13. Lambrechts, A., Jonckheere, V., Peleman, C., et al. (2006). *Journal of Cell Science*, *119*, 1570–1578. doi:10.1242/jcs.02884.
14. Birbach, A., Verkuyl, J. M., & Matus, A. (2006). *Experimental Cell Research*, *312*, 2279–2287. doi:10.1016/j.yexcr.2006.03.026.
15. Wu, N., Zhang, W., Yang, Y., et al. (2006). *Proteomics*, *6*, 6095–6106. doi:10.1002/pmic.200500321.
16. Clarke, S. R., Staiger, C. J., Gibbon, B. C., et al. (1998). *The Plant Cell*, *10*, 967–979.
17. Shurong, H., John, M. M., Michael, J. W., et al. (1996). *Plant Physiology*, *111*, 115–126. doi:10.1104/pp.111.1.115.
18. Valenta, R., Duchene, M., Pettenburger, K., et al. (1991). *Science*, *253*, 557–560. doi:10.1126/science.1857985.
19. Zuidmeer, L., Salentijn, E., Rivas, M. F., et al. (2006). *Clinical and Experimental Allergy*, *36*, 666–675. doi:10.1111/j.1365-2222.2006.02453.x.
20. Witke, W. (1998). *The EMBO Journal*, *17*, 967–976. doi:10.1093/emboj/17.4.967.
21. Song, J., Zhang, H., Liu, Z., et al. (2008). *Molecular Biology Reports*, *35*, 231–237.
22. Lambrechts, A., Verschelde, J. L., Jonckheere, V., et al. (1997). *The EMBO Journal*, *16*, 484–494. doi:10.1093/emboj/16.3.484.
23. Gieselmann, R., Kwiatkowski, D. J., Janmey, P. A., et al. (1995). *European Journal of Biochemistry*, *229*, 621–628. doi:10.1111/j.1432-1033.1995.tb20506.x.
24. Di Nardo, A. D., Gareus, R., Kwiatkowski, D., et al. (2000). *Journal of Cell Science*, *113*, 3795–3803.
25. Braun, A., Aszodi, A., Hellebrand, H., Berna, A., et al. (2002). *Gene*, *283*, 219–225. doi:10.1016/S0378-1119(01)00855-1.
26. Obermann, H., Raabe, I., Balvers, M., et al. (2004). *Molecular Human Reproduction*, *11*, 53–64. doi:10.1093/molehr/gah132.
27. Cooley, L., Verheyen, E., & Ayers, K. (1992). *Cell*, *69*, 173–184. doi:10.1016/0092-8674(92)90128-Y.
28. Verheyen, E. M., & Colley, L. (1994). *Development*, *120*, 717–728.
29. Minakhina, S., Myers, R., Druzhinina, M., et al. (2005). *BMC Cell Biology*, *6*, 32. doi:10.1186/1471-2121-6-32.
30. Zhang, Y. Z., Chen, J., Nie, Z. M., et al. (2007). *Applied Biochemistry and Biotechnology*, *136*, 327–343. doi:10.1007/s12010-007-9029-3.
31. Guindon, S., & Gascuel, O. (2003). *Systematic Biology*, *52*, 696–704. doi:10.1080/10635150390235520.
32. Guex, N., & Peitsch, M. C. (1997). *Electrophoresis*, *18*, 2714–2723. doi:10.1002/elps.1150181505.
33. Kong, L., Lv, Z., Chen, J., et al. (2007). *Biochimica et Biophysica Acta*, *1770*, 1598–1604.
34. Kenneth, J. L., & Thomas, D. S. (2001). *Method*, *25*, 402–408.
35. Metzler, W. J., Bell, A. J., Ernst, E., et al. (1994). *The Journal of Biological Chemistry*, *269*, 4620–4625.
36. Mahoney, N. M., Rozwarski, D. A., Fedorov, E., et al. (1999). *Nature Structural Biology*, *6*, 666–671. doi:10.1038/10722.
37. Polet, D., Lambrechts, A., Vandepoele, K., et al. (2007). *FEBS Letters*, *581*, 211–217. doi:10.1016/j.febslet.2006.12.013.
38. Kabsch, W., Mannherz, H. G., Suck, D., et al. (1990). *Nature*, *347*, 37–44. doi:10.1038/347037a0.
39. Flaherty, K. M., Deluca-Flaherty, C., & Mckay, D. B. (1990). *Nature*, *346*, 623–628. doi:10.1038/346623a0.
40. Staiger, C. J., Gibbon, B. C., Kovar, D. R., et al. (1998). *Trends in Plant Science*, *2*, 275–281. doi:10.1016/S1360-1385(97)86350-9.
41. Kovar, D. R., Harris, E. S., Mahaffy, R., et al. (2006). *Cell*, *124*, 423–435. doi:10.1016/j.cell.2005.11.038.
42. Witke, W. (2004). *Trends in Cell Biology*, *14*, 461–469. doi:10.1016/j.tcb.2004.07.003.
43. Valster, A. H., Vidali, L., & Hepler, P. K. (2003). *Protoplasma*, *222*, 85–95. doi:10.1007/s00709-003-0005-7.
44. Zhao, K. J., Wang, W. D., Rndo, O. J., et al. (1998). *Cell*, *95*, 625–636. doi:10.1016/S0092-8674(00)81633-5.
45. Percipalle, P., Zhao, J., Pope, B., et al. (2001). *The Journal of Cell Biology*, *153*, 229–236. doi:10.1083/jcb.153.1.229.
46. Pullmann, R. Jr., Kim, H. H., Abdelmohsen, K., et al. (2007). *Molecular and Cellular Biology*, *27*, 6265–6278. doi:10.1128/MCB.00500-07.
47. Glisovic, T., Bachorik, J. L., Yong, J., et al. (2008). *FEBS Letters*, *582*, 1977–1986. doi:10.1016/j.febslet.2008.03.004.
48. Joglekar, M. V., Parekh, V. S., Mehta, S., et al. (2007). *Developmental Biology*, *311*, 603–612. doi:10.1016/j.ydbio.2007.09.008.
49. Asangani, I. A., Rasheed, S. A., Nikolova, D. A., et al. (2008). *Oncogene*, *27*, 2128–2136. doi:10.1038/sj.onc.1210856.

50. Johnson, S. M., Grosshans, H., Shingara, J., et al. (2005). *Cell*, *120*, 635–647. doi:10.1016/j.cell.2005.01.014.
51. Chen, Y., & Gorski, D. H. (2008). *Blood*, *111*, 1217–1226. doi:10.1182/blood-2007-07-104133.
52. Yarmola, E. G., & Bubb, M. R. (2006). *Trends in Biochemical Sciences*, *31*, 197–205. doi:10.1016/j.tibs.2006.02.006.
53. Finkel, T., Theriot, J. A., Dise, K. R., et al. (1994). *Proceedings of the National Academy of Sciences of the United States of America*, *91*, 1510–1514. doi:10.1073/pnas.91.4.1510.